Available online at www.sciencedirect.com
SCIENCE DIRECT®
Electric Power Systems Research 72 (2004) 1–11
ELECTRIC POWER SYSTEMS RESEARCH
www.elsevier.com/locate/epsr

A study of the variation of synchronous machine parameters due to saturation: a numerical approach

Rafael Escarela-Perez [a,*], Tadeusz Niewierowicz [b], Eduardo Campero-Littlewood [a]

[a] *Departamento de Energia, Universidad Autonoma Metropolitana, Av. San Pablo 180, Col. Reynosa, C.P. 02200 Mexico, D.F., Mexico*
[b] *Instituto Politecnico Nacional, ESIME-SEPI, U.P. Adolfo Lopez Mateos, Edif. z-4, C.P. 07738 Mexico, D.F., Mexico*

Received 18 June 2003; accepted 5 March 2004

Available online 2 June 2004

Abstract

This paper shows the variation of the fundamental parameters of synchronous machine two-axis equivalent circuits due to magnetic saturation. The different magnetic states of the machine are obtained using finite-element magnetostatic solutions. This way the permeability patterns of the saturable parts of the machine can be stored and used in a specially designed finite-element program that outputs the standstill frequency response (SSFR) of the machine. A hybrid genetic algorithm, capable of finding global extrema is then applied to obtain the parameters of two equivalent circuit structures for the *d*-axis. The process is repeated for each magnetic state, so that the variation of parameters can be seen. The magnetic states of the machine are validated by comparing the measured open-circuit characteristic with the one calculated from the finite-element model. In order to validate the *d*-axis equivalent circuit parameters identified, they have been adopted in the simulation of a synchronous machine short-circuit and the results obtained have been compared to those calculated by a transient finite-element program.

Keywords: Standstill frequency response; Finite-element modeling; Hybrid genetic algorithm; Synchronous machines

1. Introduction

Accurate prediction of synchronous machine performance is a very important step in the design, analysis and operation of electric power systems [1]. Several approaches have been taken to model the complex behaviour of the synchronous machine: (a) two-axis equivalent circuits [2], (b) magnetic equivalent circuits [3] and (c) finite-element modelling [4]. The two-axis equivalent approach is easy to implement and requires little computer resources, but its parameters are difficult to obtain, even for the smallest (traditional) two-axis equivalent circuit [5]. The magnetic equivalent circuits have also successfully simulated steady-state and transient performance of synchronous generators [6]. These circuits can be more precise than the traditional two-axis approach, as they can portray the distributed nature of the magnetic field inside the machine with higher accuracy. However, previous knowledge of the flux paths is required to properly locate the magnetic reluctances of the model. Finite-element modelling [7] is now accepted as one of the most powerful tools to simulate synchronous generators, but computer requirements are usually high. Hence, it is not at the moment feasible to implement, for example, multi-machine stability studies with this technique. Nevertheless, it is desirable to translate the accuracy achieved with the finite-element method to the low-order two-axis models. Some work has been made in this direction [8], where finite-element simulations are used to obtain two-axis circuit parameters. Advances in system identification techniques have allowed the determination of two-axis high-order equivalent circuits from actual tests [9], especially from the standstill frequency response test (SSFR). However, the optimization problem involved with the identification process is usually performed using deterministic methods that can get stuck into local extrema. This may lead to wrong conclusions about the meaning and utilization of the identified parameters [10]. The incorporation of hybrid genetic algorithms into the optimization problem has alleviated this drawback

* Corresponding author. Tel.: +52 55 5318 9584; fax: +52 55 5394 7378.
E-mail address: r.escarela@ieee.org (R. Escarela-Perez).

0378-7796/$ – see front matter © 2004 Elsevier B.V. All rights reserved.
doi:10.1016/j.epsr.2004.03.001

(see Refs. [8,11]). As a result, it is now possible to perform more reliable comparisons between parameters of different circuit structures and to obtain the right high-order equivalent circuit for a given machine. One of the problems associated with the standard SSFR test is that magnetic saturation cannot be accounted for in the test itself and corrections are usually performed in the calculated magnetizing inductances [12].

There has been a continuous interest nevertheless in the impact of magnetic saturation in the circuit parameters of synchronous generators. Several methods have been proposed to achieve this goal through saturation factors [13–15], by which cross-magnetizing effects can be accounted for. These techniques, although based on sound physical and theoretical basis, are at most a good approximation to reality, since it is assumed that saturation merely affects the magnetizing inductances of the machine. However, it is worth mentioning that these approximations usually lead to better results, that is, the matching between test and simulation results is normally improved [14].

The results presented in [16,17] represent major steps in the formal determination of the influence that saturation has on the dynamic circuit parameters of two-axis synchronous machines models using the SSFR test. The studies performed in these references are based on actual SSFR tests, where it was possible to perform experiments at different magnetization levels. Estimated results [16] showed that saturation has an influence on most circuit parameters and that the main part of saturation could actually be captured by the magnetization main inductances.

This paper shows the application of finite-element techniques to assess the impact of saturation in the circuit parameters of synchronous generator models. This numerical approach attempts to complement the experimental work presented in [16,17], as an experimental approach is probably not realistic in high-power machines [16] due to the required currents to achieve saturation. In this work, a representative 150 MVA, 120 MW, 50 Hz turbine generator is analyzed to determine the parameters of two-axis equivalent circuits. The open-circuit characteristic is first simulated to obtain different magnetic states (saturation levels) of the machine, which are then used to obtain the SSFR of the machine for each state. A hybrid genetic algorithm is applied to determine the circuit parameters. This leads to a meaningful comparison between the different sets of parameters, as deterministic methods may lead to local extrema. Problems associated with actual tests are avoided by numerically determining the magnetic state and SSFR of the machine.

2. Calculation of magnetic saturation

The determination of the machine saturated condition is readily established as a two-dimensional current-driven problem [7] and it is solved using a simple finite-element magnetostatic program. The basic equation that must be solved in the rotor reference frame is [7]

$$\frac{\partial}{\partial x}\left(\nu\frac{\partial A_z}{\partial x}\right)+\frac{\partial}{\partial y}\left(\nu\frac{\partial A_z}{\partial y}\right)=-J_z \tag{1}$$

where A_z and J_z are the z-components of the magnetic vector potential and current density, respectively. These quantities are always directed along the axial direction of the machine for a two-dimensional representation of synchronous machines, and ν represents the reluctivity of matter. Eq. (1) is totally specified when boundary conditions (Dirichlet, Neumann and Periodic) are given. Finite-element discretization of (1) leads to a non-linear system of equations, which can be written as

$$[S]\{A\}=\{I\} \tag{2}$$

where $[S]$ is a matrix that is a direct consequence of the left-hand side of (1). It embodies the geometry information of the machine as well as its electric and magnetic properties. $\{I\}$ is a vector of known injected currents at element nodes and it results from the right-hand side of (1). $\{A\}$ is a vector of magnetic vector potentials at element nodes. The reluctivities of each finite element are stored to be used in the finite-element SSFR calculation. Fig. 1 shows the comparison between test and finite-element results. It can be seen that a good match is achieved. This validates the magnetostatic finite-element computation and it also provides confidence in the different calculated reluctivity patterns of the machine. These magnetic states (from linear to saturated condition) are used for evaluating the impact of saturation on the fundamental parameters of two-axis equivalent circuits.

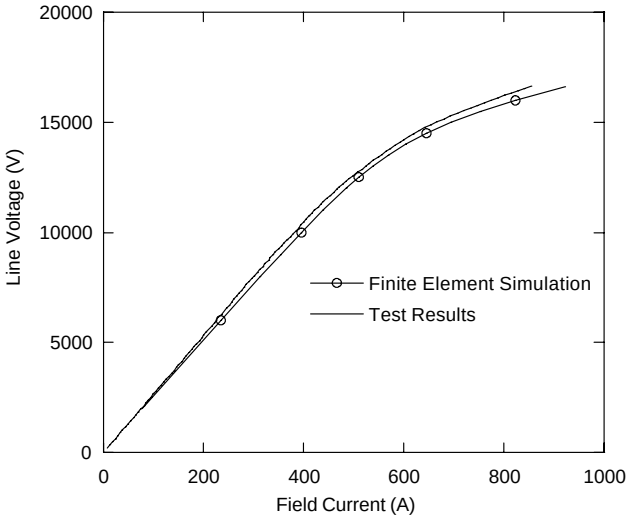

Fig. 1. Open-circuit Characteristic. Finite-element and test results.

3. SSFR calculation

The methodology used in this work for calculating the SSFR of the machine by the finite-element method is fully

described in [18], but a brief discussion of the basic equations is given here for the sake of completeness. The basic relationship that must be solved in the frequency domain is given by [11]:

$$\frac{\partial}{\partial x}\left(\nu\frac{\partial \tilde{A}_z}{\partial x}\right)+\frac{\partial}{\partial y}\left(\nu\frac{\partial \tilde{A}_z}{\partial y}\right)=-\tilde{J}_z+\mathrm{j}\omega\sigma\tilde{A}_z \tag{3}$$

where ω is the electrical angular frequency and σ is the conductivity of matter. The symbol $\sim$ (on top of variables) denotes complex quantities/phasors. The second term of the right-hand side of (3) represents the eddy currents induced in the rotor body. The field winding must be shortened during the test, leading to a problem where the field current is unknown before the solution and cannot be pre-specified in (3). As a result, the circuit equation of the field winding must be solved simultaneously with (3) [18] to obtain a consistent system of equations. This extra equation is given by

$$\tilde{u}_\mathrm{f}=\tilde{i}_\mathrm{f}(r_\mathrm{f}+\mathrm{j}\omega L_\mathrm{endf})+\tilde{E}_\mathrm{f} \tag{4}$$

where $\tilde{u}_\mathrm{f}$ is the voltage at the field winding terminals, r_f and L_endf are the resistance and end-winding inductance of the field winding. $\tilde{E}_\mathrm{f}$ is the internal voltage generated within the finite-element domain of the field winding, whereas $\tilde{i}_\mathrm{f}$ is the complex current circulating in the field winding. The short-circuit condition required by the SSFR [12] is readily incorporated by setting $\tilde{u}_\mathrm{f}=0+\mathrm{j}0$. Eqs. (3) and (4) are complemented with appropriate boundary conditions (Dirichlet, Neumann and Periodic). Finite-element discretization of (3) and (4) leads to a linear system (if the permeability characteristics of matter are considered invariant) of equations, which can be written as [18]

$$\begin{bmatrix}[S] & \{N_\mathrm{f}\}\\ \{N_\mathrm{f}\}^\mathrm{T} & \tilde{K}\end{bmatrix}\begin{Bmatrix}\tilde{A}\\ -\tilde{i}_\mathrm{f}\end{Bmatrix}=\begin{Bmatrix}\tilde{I}\\ 0+\mathrm{j}0\end{Bmatrix} \tag{5}$$

where $\{N_\mathrm{f}\}$ is a winding vector [18], while $\tilde{K}$ is a complex constant quantity that is obtained from (4). The finite-element model substitutes the actual three phase stator by two sinusoidally distributed windings [18]. The complex solution of the system of equations (for a given frequency) are processed to obtain the complex values of three transfer functions that completely characterize [19] the d-axis two-port network of the machine:

$$X_d(\mathrm{j}\omega)=\left.\frac{\omega_0\tilde{\lambda}_d}{\tilde{i}_d}\right|_{q\text{-asix stator winding open and field winding shorted}}+\text{leakage overhang term} \tag{6a}$$

$$\frac{\mathrm{j}\omega G(\mathrm{j}\omega)}{\omega_0}=\left.\frac{\tilde{i}_\mathrm{f}}{\tilde{i}_d}\right|_{q\text{-axis stator winding open and field winding shorted}} \tag{6b}$$

$$X_{\mathrm{af}0}(\mathrm{j}\omega)=\left.\frac{\omega_0\tilde{\lambda}_\mathrm{f}}{\tilde{i}_d}\right|_{q\text{-axis stator and field winding open}} \tag{6c}$$

where $\tilde{\lambda}_d$ and $\tilde{\lambda}_\mathrm{f}$ are the flux linkages with the d-axis and field windings, respectively. ω_0 is the nominal electrical angular frequency. $X_d(\mathrm{j}\omega)$ is the d-axis operational reactance, $\mathrm{j}\omega G(\mathrm{j}\omega)/\omega_0$ is the ratio of the d-axis stator current to the field current. $X_{\mathrm{af}0}(\mathrm{j}\omega)$ is the mutual operational reactance between the d-axis and field windings.

The q-axis one-port network only requires one transfer function; in this case the q-axis operational reactance $X_q(s)$. It is worth mentioning here that the finite-element program solves the complex version of the diffusion equation [7,18] using a constant reluctivity pattern supplied by the user. The reluctivity patterns calculated in Section 2 (16 points were obtained) were used to obtain the SSFR of the machine under different levels of saturation.

Fig. 2 shows the variation of magnitude of the d-axis operational reactance due to saturation. Curves are plotted for 16 different magnetization levels, which go from the linear condition to the saturated one. It can be observed that as the machine saturates the magnitude of the d-axis operational inductance decreases. This is an expected result since saturation increases the reluctivity of the machine components. However, it is very interesting to note that the 16 curves converge to the same value as frequency increases. This can be readily explained since the magnetic field is screened from the rotor body as the frequency steps up and it is, therefore, forced into leakage paths with nearly constant permeability patterns. Fig. 3 shows the variation of the phase angle of the

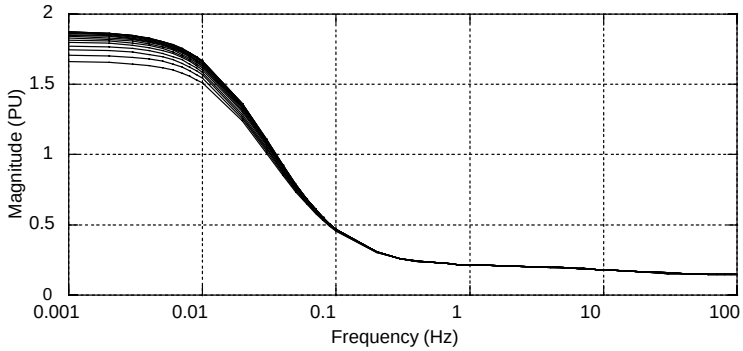

Fig. 2. Magnitude of the d-axis operational reactance $X_d(s)$ at different magnetization levels.

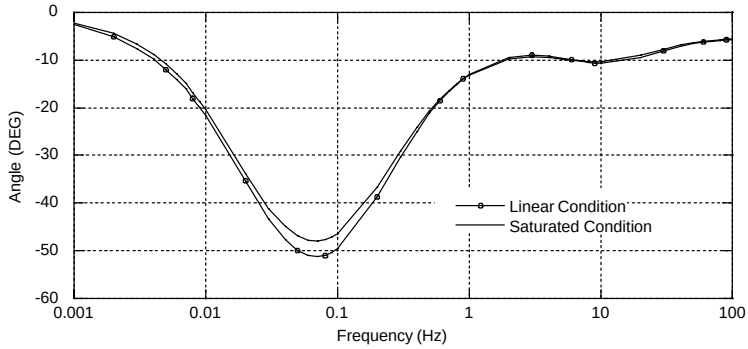

Fig. 3. Angle of the d-axis operational reactance $X_d(s)$. Linear and saturated conditions.

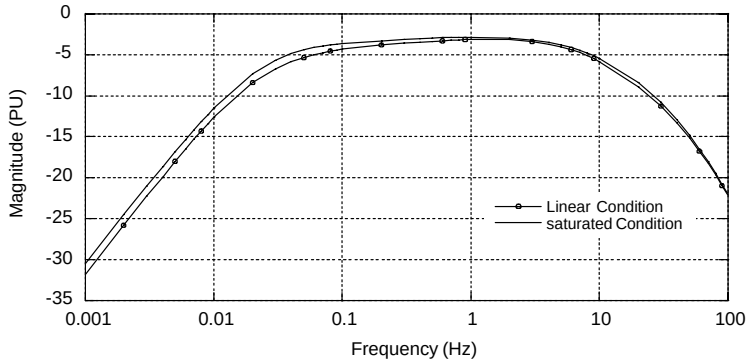

Fig. 4. Magnitude of the ratio of the d-axis stator current to field current $j\omega G(j\omega)/\omega_0$. Linear and saturated conditions.

d-axis operational reactance, only for the linear case (lowest excitation level considered in this work) and for the most saturated case, so as to avoid confusion with overcrowded curves in the same graph. Figs. 4–7 show the limiting cases for the magnitudes and angles of the ratio of the d-axis stator current to field current transfer function and mutual operational reactance between the d-axis and field winding. It can be seen that saturation mainly affects the magnitudes of the three transfer functions. The phase angles are also affected but the impact of saturation is smaller. It is also remarkable to note that the saturation effect is stronger at low frequencies. This may explain the results of [16], where it is concluded that the main part of saturation can be captured by the magnetization inductances, as at high frequencies the values of the transfer functions converge to the same value. The angle differences observed in the figures are most likely produced by the non-uniform distribution of saturation of the iron cores. Figs. 8 and 9 show the variation of the q-axis operational reactance. The magnitude of this transfer function is mainly affected by saturation at low frequencies, but the phase angle is affected in most frequencies. This result may be explained by the fact that as saturation in the d-axis (calculated from the open-circuit characteristic) becomes important, not only the d-axis reluctance is modified but also the q-axis magnetic path for each magnetic state is changed.

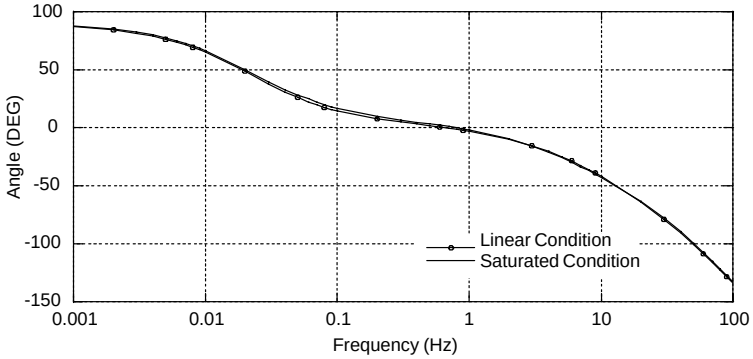

Fig. 5. Angle of the ratio of the d-axis stator current to field current $j\omega G(j\omega)/\omega_0$. Linear and saturated conditions.

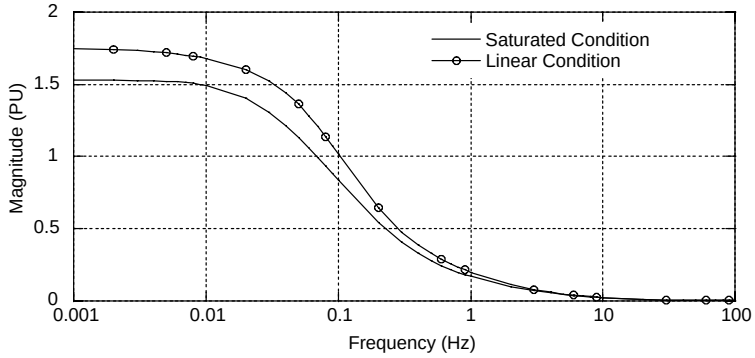

Fig. 6. Magnitude of the operational reactance $X_{af0}(j\omega)$. Linear and saturated conditions.

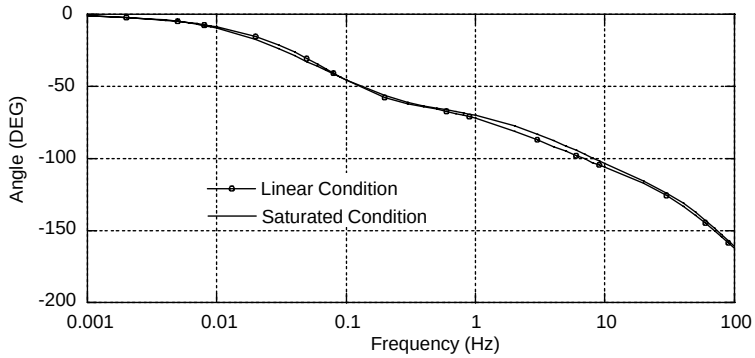

Fig. 7. Angle of the operational reactance $X_{af0}(j\omega)$. Linear and saturated conditions.

4. Two-axis equivalent circuit parameters

The SSFR test [12] is mainly performed to obtain the parameters of two-axis equivalent circuits. Fig. 10 shows an established equivalent circuit structure [2], which is often employed for determining circuit parameters. L_a and r_a are the leakage inductance and resistance of the stator windings. L_{md} is the magnetizing inductance of the d-axis. $L_{kf1}, L_{kf2}, \ldots, L_{kfn}$, are leakage differential inductances of the rotor circuits. $L_{d1}, L_{d2}, \ldots, L_{dn}$ are the leakage inductances of the d-axis rotor damper windings and $r_{d1}, r_{d2}, \ldots, r_{dn}$ are their respective resistances, r_f and L_f are the resistance and leakage inductance of the field winding, while n is the number of damper branches used in the d-axis. The q-axis equivalent circuit can be obtained from Fig. 10 by eliminating the differential leakage inductances and the field winding branch (letter q substitutes subscript d). The d-axis system identification problem can be set-up as [11]

$$FF = \sum_{j=1}^{N}\sum_{i=1}^{3}\left[(\bar{M}_i(\bar{\theta}_d) - \bar{M}_i^d)^2 + (\Phi_i(\bar{\theta}_d) - \bar{\Phi}_i^d)^2\right] \quad (7)$$

so that:

$$\min_{\theta} FF \quad (8)$$

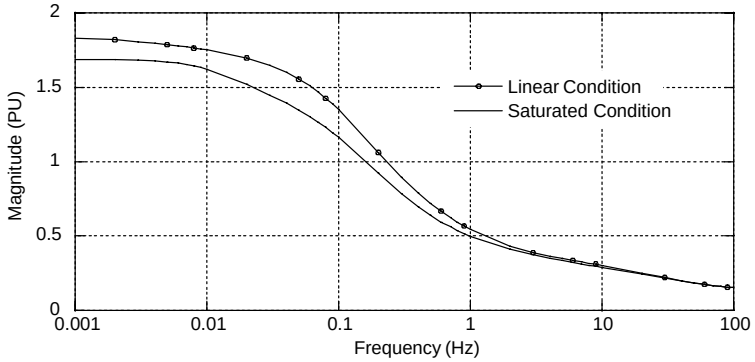

Fig. 8. Magnitude of the q-axis operational reactance $X_q(j\omega)$. Linear and saturated conditions.

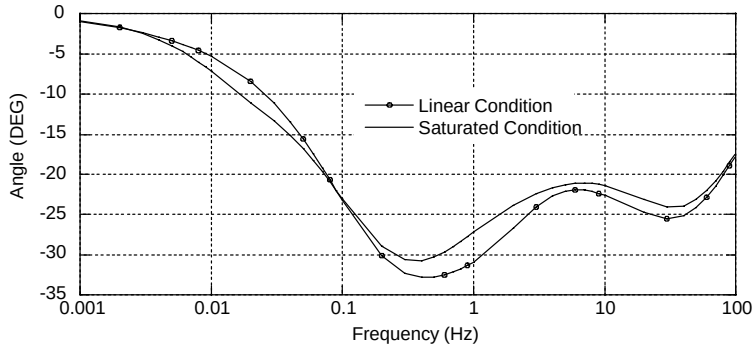

Fig. 9. Angle of the q-axis operational reactance $X_q(j\omega)$. Linear and saturated conditions.

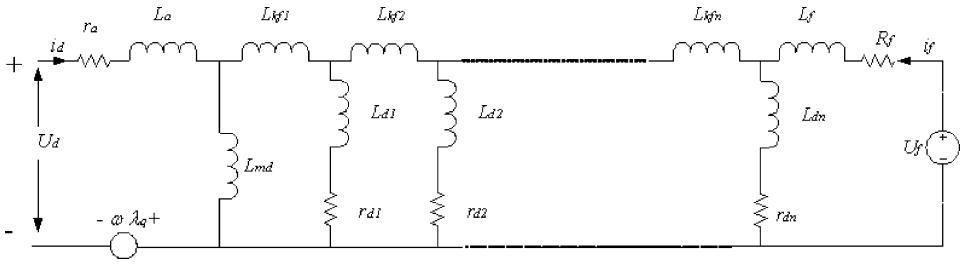

Fig. 10. Two-axis equivalent circuit of the synchronous machine.

The following definitions apply:

$$M_{ij}^{d} \in \bar{M}_{i}^{d} \subset \bar{M}^{d} \quad \forall_j$$

is the set of observable magnitudes of the d-axis transfer functions.

$$\Phi_{ij}^{d} \in \bar{\Phi}_{i}^{d} \subset \bar{\Phi}^{d} \quad \forall_j$$

is the set of observable d-axis phase angles.

$$M_{ij} \in \bar{M}_{i} \subset \bar{M} \quad \forall_j$$

is the set of calculated magnitudes of the d-axis equivalent circuit.

$$\Phi_{ij} \in \bar{\Phi}_{i} \subset \bar{\Phi} \quad \forall_j$$

is the set of calculated phase angles of the d-axis equivalent circuit and $\bar{\theta}$ is the set of parameters that must be identified [11]. A hybrid genetic algorithm [8,11] was used to determine the circuit parameters of two structures: (a) one-damper winding and (b) five-damper windings. The one-damper circuit is of interest since it is widely used in power system calculations. However, its ability to reproduce the SSFR is not very good [8]. The five-damper circuit is able to reproduce the SSFR of the machine in a nearly perfect way [11]. The way to determine the right number of damper branches needed to achieve this accuracy is described in [11].

4.1. One-damper d-axis circuit

Fig. 11 shows the saturation variation of the d-axis magnetizing reactance X_{md}, which decreases as the excitation levels rise. This behaviour is well known and it does not need further explanation. However, it should be noted that this reactance was calculated using the finite-element procedure described in [8] and that this reactance is assumed to be known during the identification of two-axis circuit parameters. This also applies for the stator leakage reactance (shown in Fig. 12), which was calculated [8] using the winding vector concept [20]. This explains the smooth behaviour of their variation. These reactances are independent of the two-axis equivalent circuit structures used in the identification process and they are, therefore, the same for the two equivalent circuits considered here. The field to armature turns ratio was calculated using the finite-element procedure described in [8]. It was very interesting to find that this parameter remains

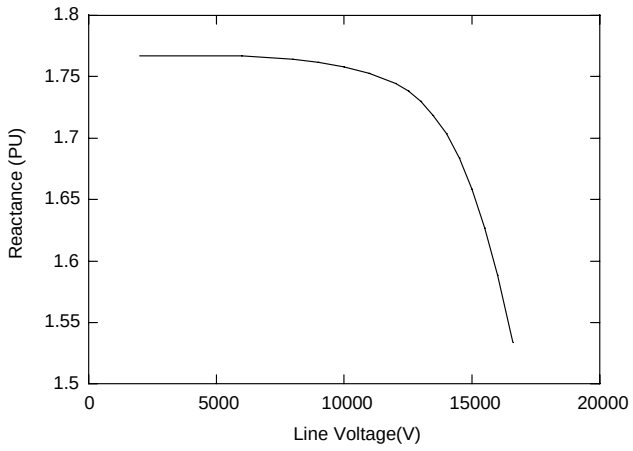

Fig. 11. Variation of the magnetizing reactance X_{md} due to saturation.

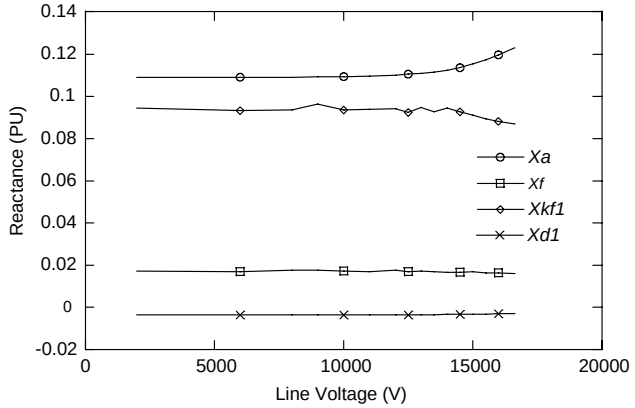

Fig. 12. Variation of reactance parameters for the one-damper *d*-axis circuit.

nearly unaffected by saturation, as it only changes 0.8% from the unsaturated case to the saturated one. The increase of the stator leakage reactance can look surprising, but it may be explained by the fact that this reactance was calculated using sinusoidally distributed winding vectors [18], which tend to neglect harmonic effects. In other words, the leakage reactance calculated here is a very good approximation of the real value, but it is not the exact one. Nevertheless, the variation of this reactance indicates that saturation does have an effect on this parameter. It should be emphasized that the use of sinusoidal winding vectors perfectly comply with the theory of two-axis equivalent circuits [21] and, hence, the stator leakage reactance thus calculated can be safely used in the dynamic simulation of synchronous machines as shown in [18]. If a more accurate value of this reactance is required, the finite-element procedure of [22] can be used. Fig. 12 shows the variation with voltage of the remaining reactances of the one-damper *d*-axis circuit. Although the variation in each case may seem small, the damper leakage reactance X_{d1} changes 22% from the lowest excitation level (used in this work) to the highest one. The differential leakage reactance X_{kf} shows a corresponding 8% variation, while the field

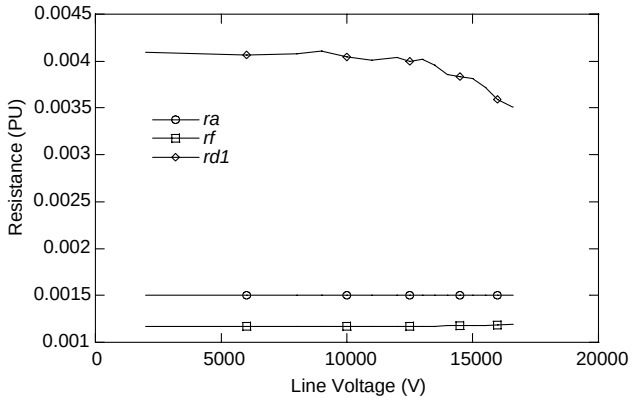

Fig. 13. Variation of resistance parameters for the one-damper *d*-axis circuit.

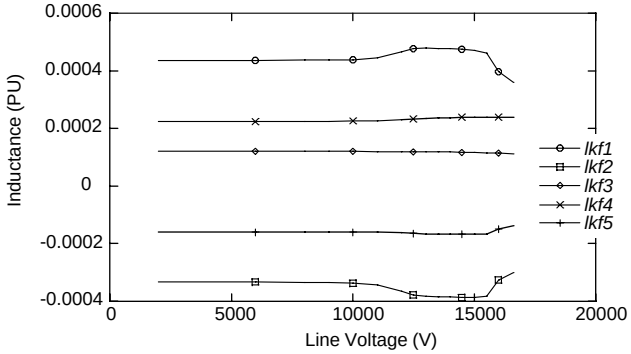

Fig. 14. Variation of inductance parameters for the five-damper *d*-axis circuit (L_{kf} terms).

winding leakage reactance changes 7%. Fig. 13 shows the variation of the *d*-axis circuit resistances, where it can be observed that the armature resistance remains constant, since it is assumed to be known during the identification process (see Refs. [8,11] for more details). It can also be seen that the field winding resistance remains nearly constant for all the excitation levels with a maximum change of 1.6%. The damper winding resistance shows a larger variation, of about 14%.

4.2. Five-damper d-axis circuit

The inductance variation with voltage of the five-damper *d*-axis circuit is shown in Figs. 14–16. The differential leakage inductance L_{kf1} shows the bigger variation with a change of 17% from the linear case to the saturated one, whereas L_{kf4} has the smallest variation of the leakage differential-inductance set, only 6.8%. The leakage inductance L_{d1} modifies its unsaturated value by 61%, while L_{d4} is the inductance showing the smallest variation within the leakage-inductance set with a change of 12.8% (see Fig. 16). The damper resistance variation is shown in Fig. 17, where the largest variation (45%) is given by r_{d1}, while the smallest deviation (2.6%) is presented by r_{d2}. It can be observed that saturation changes are bigger for the five-damper *d*-axis circuit structure than for the one-damper circuit. It is also important to observe that some of the leakage inductances are negative. A discussion of the physical meaning that these

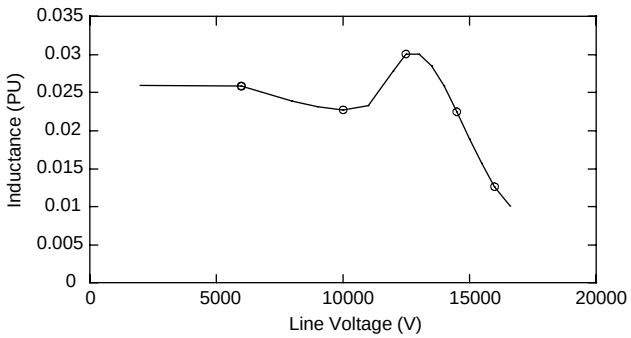

Fig. 15. Variation of inductance L_{d1} for the five-damper *d*-axis circuit.

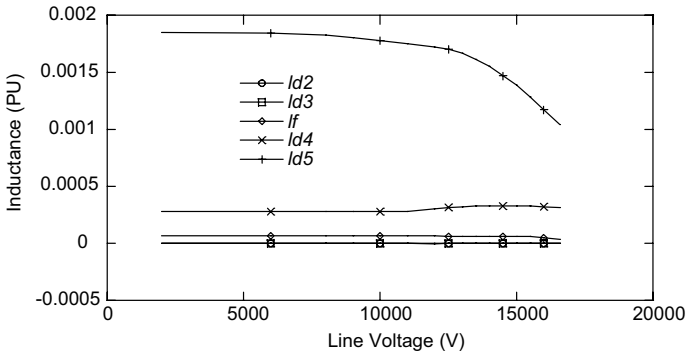

Fig. 16. Variation of inductance parameters for the five-damper d-axis circuit (L_f and L_d terms).

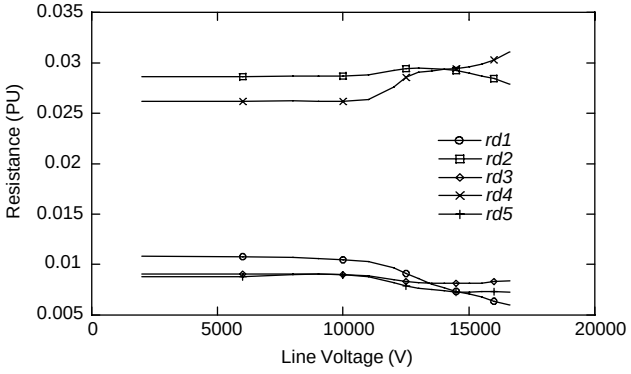

Fig. 17. Variation of resistance parameters for the five-damper d-axis circuit.

parameters may have is given in [8], where it is shown that false conclusions can be obtained from parameters obtained from frequency response tests. The main reason is that several sets of parameters can give good fitting characteristics since they can be produced by local minima. Moreover, the identification problem can be constrained to positive values of inductance [8], avoiding negative values and also obtaining very good fitting characteristics. So, it is very difficult (even impossible) to give a physical meaning to each parameter. Perhaps, it is better to say that a set of parameters is the result of a mathematical process of identification, which can accurately reproduce the frequency response of the machine. In this work, the identification problem is not constrained and was solved using a hybrid genetic algorithm, which gives the global minimum, that is, the best set of parameters that can reproduce the machine SSFR.

5. Impact of variation of parameters

The substantial changes of d-axis parameters due to saturation may lead to the conclusion that two-axis models need to consider these saturation alterations during numerical simulations. However, some important aspects must be considered before reaching definite conclusions. The leakage inductance changes may seem large but when the fundamental inductances (that is the self and mutual inductances between machine windings, see Ref. [2]) are calculated from the magnetizing and leakage inductances, it can be concluded that the changes are not exaggeratedly big. The reason for this is that the magnetizing inductance is always used to calculate the self and mutual inductances by adding to it leakage inductance values, which are always much smaller than the magnetizing inductance value. For instance, the self-inductance of the field winding is given by the sum of the magnetizing inductance, the leakage inductance L_f and all differential leakage inductances of the equivalent circuit [2]. For the lowest excitation level and the five-damper circuit considered in this work it has a per-unit value of 5.98E−3, while the per-unit value for the most saturated case is 5.19E−3. This implies a 13.21% change from the linear to the saturated case. It is important to note that the magnetizing inductance changes 13.17% from the unsaturated value to the saturated one. In other words, the magnetizing inductance is responsible for the main part of the change, even though the leakage inductance L_f changes nearly 50%. Similar results can be found for all the other self and mutual inductances of the machine. Another important aspect to be considered is that a large change of one particular circuit parameter may not have a strong impact in the electrical characteristics of the synchronous machine. This has been shown in Ref. [8], where the values of the fitness function used in the d-axis parameter identification process are not greatly affected by large changes of some of the parameters. This means that the data used to identify the parameters can be neatly reproduced, notwithstanding the fact that some of the parameters suffer large variations or even change sign [8]. It is important to mention that the changes analyzed in [8] were artificially produced to study the sensitivity of the identification fitness function, but they clearly give insight into the impact of parameter variations.

The previous argumentation can only be useful when the impact of parameter variation is indeed small in numerical simulations of synchronous machines. A short-circuit condition of the generator considered in this work was simulated with an established transient finite-element program [23],

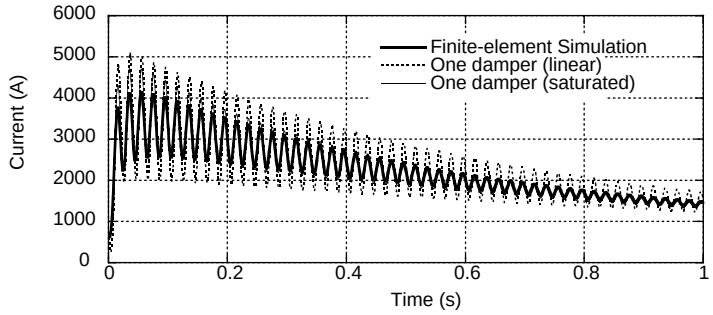

Fig. 18. Short-circuit field current. Finite-element and one-damper circuit simulations.

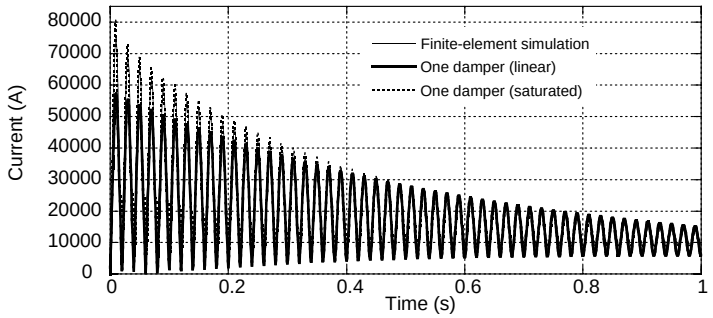

Fig. 19. Short-circuit stator current. Finite-element and one-damper circuit simulations.

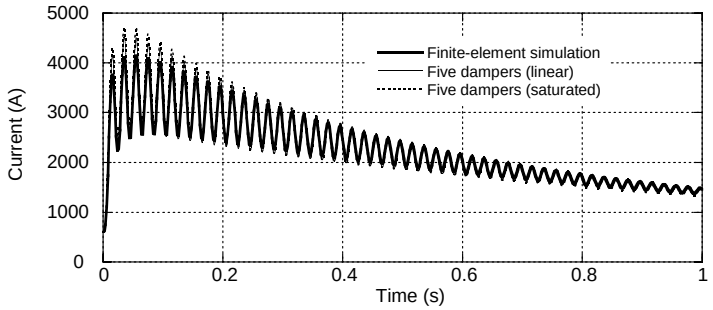

Fig. 20. Short-circuit field current. Finite-element and five-damper circuit simulations.

that is, a finite-element code already validated against test results. It is important to mention that the SSFR finite-element code is completely independent of the finite-element transient one. The initial (open-circuit) condition of the machine was used to calculate the magnetizing inductances, the stator leakage inductance and the field-to-armature turn ratio. The open-circuit magnetic state was also used to calculate the *q*-axis SSFR of the machine. As a result, it was possible to identify *q*-axis circuit parameters, which were kept unchanged through all the numerical simulations performed in this work. It is important to note that the impact of the *q*-axis parameters is small, since the no-load

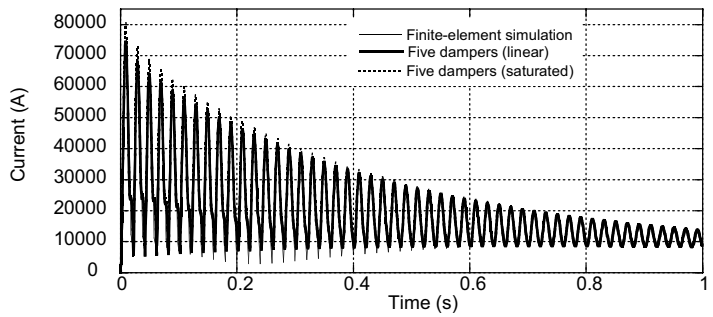

Fig. 21. Short-circuit stator current. Finite-element and five-damper circuit simulations.

short-circuit condition analyzed here involves a transient condition that is mainly developed in the *d*-axis. In order to study only the effect of the rotor *d*-axis parameters, the transient finite-element simulation was performed keeping the reluctivity pattern of the machine constant (as calculated for the open-circuit condition). This implies that the stator leakage inductance and the magnetizing inductances remain constant during the transient condition, so that the variation of magnetizing inductances is no longer a variable during the numerical simulations. Two simulations were performed for each of the *d*-axis equivalent circuit structures considered in this work, using the following sets of *d*-axis rotor circuit parameters: (a) lowest excitation level and (b) highest excitation level. Figs. 18 and 19 show the comparison of the finite-element short-circuit currents with the corresponding one-damper two-axis circuit simulations. Fig. 18 shows the short-circuit current of the field winding, whereas Fig. 19 depicts the stator short-circuit current. The circuit responses, which correspond to the one-damper two-axis circuit simulations, show less damping than the finite-element one. Both sets of two-axis parameters can be seen to give very similar results. These figures also evidence the limitations of one-damper *d*-axis circuit models to properly reproduce the transient behaviour of the generator. Figs. 20 and 21 show the comparison between finite-element results and the five-damper *d*-axis circuit simulations. It is interesting to see that a five-damper equivalent circuit has a much better capability to model the synchronous machine, no matter which set of *d*-axis rotor circuit parameters is used (unsaturated or saturated) in the circuit simulations. It is pretty clear that the saturation influence is small when compared with the impact of the number of branches used to simulate the machine. Moreover, the difference between simulation results of two corresponding sets is moderately small.

6. Conclusions

In this work, an analysis of the impact of variation of the *d*-axis equivalent circuit parameters on synchronous machine transient behaviour determination has been presented. The determination of parameters was performed using a finite-element model for a large turbine generator and a hybrid genetic algorithm, leading to sets of circuit parameters that can be safely compared. The reason for this is that the circuit parameters represent global solutions of the system identification problem. The determination of parameter variations due to saturation was possible, since the magnetic/reluctivity states of the machine were available from finite-element simulations, which were validated against test results. These magnetic states were fed to a special finite-element code designed to obtain the SSFR of the machine for each operating point. As a result, two-axis circuit parameters were obtained using a three-transfer function approach, with a hybrid genetic algorithm as the optimization solver. The variation for some parameters was found to be large, having changes bigger than 50% in some cases. These results tend to confirm the experimental findings of Refs. [16,17], obtained with laboratory (small) machines. It must be emphasized here that experimental work may not be realistic in high-power machines due to the high currents required to reach saturation. Hence, numerical approaches seem to represent the best way to study the effect of saturation on large synchronous generators. Although rotor *d*-axis circuit parameters exhibit large changes, it was possible to show that their impact is not as big as it seems. Actually, it was observed that the most important impact of saturation is mainly reflected in the magnetizing inductances. This complies with the traditional methods, which take saturation into account by modifying these parameters alone. It was also very interesting to find that the number of damper branches is more important in numerical simulations of synchronous generators than the influence of rotor circuit parameter variations. Nevertheless, it is desirable to provide power system analyzers with a single set of parameters. A global estimated model of the machine can be found [16], but it is thought that a more simple way to define a unique set of circuit parameters is using the magnetic state of the open-circuit nominal operating point of the machine to obtain the two-axis circuit parameters. This is justified by the fact that parameters from the lowest excitation level set give similar results to those from the most saturated one. Although the results are not exactly the same, the work of taking into consideration these variations in two-axis models is not worthwhile.

Acknowledgements

This work was supported by the National Council of Science and Technology of Mexico (CONACYT).

References

[1] P. Kundur, Power System Stability and Control, McGraw-Hill, 1994.
[2] I. Kamwa, R. Wamkeue, X. Dai-Do, General approaches to efficient *d–q* simulation and model translation for synchronous machines: a recap, Electric Power Syst. Res. 42 (3) (1997) 173–180.
[3] S.R. Slemon, An equivalent circuit approach to analysis of synchronous machines with saliciency and saturation, IEEE Trans. Energy Conversion 5 (3) (1990) 538–545.
[4] J.P. Sturgess, M. Zhu, D.C. Macdonald, Finite-element simulation of a generator on load during and after a three-phase fault, IEEE Trans. Energy Conversion 7 (4) (1992) 787–793.
[5] G. Shackshaft, New approach to the determination of synchronous-machine parameters from tests, IEE Proc. 121 (11) (1974) 1385–1392.
[6] M.J. Carpenter, D.C. Macdonald, Circuit representation of inverter-fed synchronous motors, Trans. Energy Conversion 4 (3) (1989) 531–537.
[7] P.P Silvester, R.L. Ferrari, Finite Elements for Electrical Engineers, 3rd ed., Cambridge University Press, 1990.

[8] R. Escarela-Perez, T. Niewierowicz, E. Campero-Littlewood, Synchronous machine parameters from frequency-response finite-element simulations and genetic algorithms, IEEE Trans. Energy Conversion 16 (2) (2001) 198–203.
[9] R. Wamkeue, I. Kamwa, X. Dai-Do, A. Keyhani, Iteratively reweighted least squares for maximum likelihood identification of synchronous machine parameters from on-line tests, IEEE Trans. Energy Conversion 14 (2) (1999) 159–166.
[10] I. Kamwa, P. Viarouge, On equivalent circuit structures for empirical modeling of turbine-generators, IEEE Trans. Energy Conversion 9 (3) (1994) 579–592.
[11] T. Niewierowicz, R. Escarela-Perez, E. Campero-Littlewood, Hybrid genetic algorithm for the identification of high-order synchronous machine two-axis equivalent circuits, Comput. Elect. Eng. 29 (4) (2003) 505–522.
[12] IEEE, Guide for Test Procedures for Synchronous Machines, IEEE Std. 115, 1995.
[13] S.A. Tahan, I. Kamwa, A two factor saturation model for synchronous machines with multiple rotor circuits, IEEE Trans. Energy Conversion 10 (4) (1995) 609–616.
[14] H. Hirayama, Practical detailed model for generators, IEEE Trans. Energy Conversion 10 (1) (1995) 105–110.
[15] A.M. El-Serafi, J. Wu, Determination of the parameters representing the cross-magnetizing effect in saturated synchronous machines, IEEE Trans. Energy Conversion 8 (3) (1993) 333–342.
[16] J. Verbeeck, R. Pintelon, P. Lataire, Influence of saturation on estimated synchronous machine parameters in standstill frequency response tests, IEEE Trans. Energy Conversion 15 (3) (2000) 277–283.
[17] G. Ahrabian, A.M. El-Serafi, Identification of the synchronous machine parameters under magnetic saturated conditions using stand still frequency response test, in: Proceedings of the Canadian Conference on Electrical and Computer Engineering, vol. 1, 2001, pp. 545–550.
[18] R. Escarela-Perez, E. Campero-Littlewood, T. Niewierowicz, Efficient finite element computation of synchronous machine transfer functions, IEEE Trans. Mag. 38 (2) (2002) 1245–1248.
[19] I. Kamwa, P. Viarouge, H. Le-Huy, E.J. Dickingson, Three-transfer approach for building phenomenological models of synchronous machines, IEE Proc.-Gener. Transm. Distrib. 141 (2) (1994) 89–98.
[20] P.J. Turner, Finite-element simulation of turbine-generator terminal faults and application to machine parameter prediction, IEEE Trans. Energy Conversion 2 (1) (1987) 122–131.
[21] B. Adkins, R.G. Harley, The General Theory of Alternating Current Machines, Chapman & Hall, London, 1975.
[22] J.C. Flores, G.W. Buckley, G. Mcpherson, The effects of saturation on the armature leakage reactance of large synchronous machines, Trans. Power Apparatus Syst. 103 (3) (1984) 593–600.
[23] R. Escarela-Perez, D.C. Macdonald, A novel finite-element transient computation of two-axis parameters of solid-rotor generators for use in power systems, IEEE Trans. Energy Conversion 13 (1) (1998) 49–54.